

Noise adaptive switching median-based filter for impulse noise removal from extremely corrupted images

A. Fabijańska D. Sankowski

Department of Computer Engineering, Technical University of Lodz, 18/22 Stefanowskiego Street, 90-924 Lodz, Poland
E-mail: an_fab@kis.p.lodz.pl

Abstract: In this study an approach to impulse noise removal is presented. The introduced algorithm is a switching filter which identifies the noisy pixels and then corrects them by using median filter. In order to identify pixels corrupted by noise an analysis of local intensity extrema is applied. Comprehensive analysis of the algorithm performance [in terms of peak signal-to-noise ratio (PSNR) and Structural SIMilarity (SSIM) index] is presented. Results obtained on wide range of noise corruption (up to 98%) are shown and discussed. Moreover, comparison with well-established methods for impulse noise removal is provided. Presented results reveal that the proposed algorithm outperforms other approaches to impulse noise removal and its performance is close to ideal switching median filter. For high noise densities, the method correctly detects up to 100% of noisy pixels.

1 Introduction

During acquisition or transmission digital images often get affected by noise. It manifests itself as erroneous intensity fluctuations which stem from imperfections of imaging devices and transmission channels [1].

Noise can seriously affect quality of images. It causes degradation of image spatial resolution, loss of image details and distortion of important image features. Therefore it is essential to correct corrupted pixels before the main processing.

The numerous approaches to noise reduction have been proposed. They differ depending on the type of noise. In this paper techniques for impulse noise removal are considered. They aim at suppressing noise while preserving detailed image information and the integrity of edges at the same time.

The most popular approach for impulse noise removal is standard median filter (SMF) [2–4]. Applied to greyscale images, SMF is a neighbourhood intensity-ranking algorithm. Each pixel in the output image equals to the median intensity of its closest neighbours in the original image. The size of the neighbourhood is determined by squared, sliding window, which passes through the whole image pixel by pixel [5, 6].

Regardless its popularity, there are drawbacks to median filtration [7]. First of all it compromises details and blurry an image. Moreover it falters when impulse noise density becomes high. Especially edge jitter can be observed then [8]. It is because SMF is performed uniformly across whole image and modifies both corrupted and uncorrupted pixels.

The noise adaptive approach presented in this paper reduces number of pixels subjected to median filtration to

those identified as corrupted ones while leaving remaining pixels unchanged. The proposed impulse detection method based on analysis of local intensity extrema detects noisy pixels with accuracy close to 99% for a wide range of noise densities. In consequence, corrupted pixels can be effectively corrected while preserving the detailed image information at the same time.

This paper is arranged as follows. First, in Section 2 noise model considered in this work is defined. Next, in Section 3 a short review of existing techniques for impulse noise removal is given. Section 4 describes the proposed filter for image denoising in detail. This is followed in Section 5 by definitions of image fidelity measures used to quantify the results obtained by the proposed algorithm. Finally, in Sections 6–8 results of extensive simulations conducted on images under a wide range of noise corruptions and their comparison with well-established methods for impulse noise removal are presented, discussed and concluded, respectively.

2 Noise model

Several types of noise have been defined [1]. In this paper the impulse noise is considered. In case of images corrupted by this kind of noise, intensity of the pixel x_{ij} at location (i, j) is described by the probability density function given by the following equation

$$f(x_{ij}) = \begin{cases} p_a & \text{for } x_{ij} = a \\ 1 - p & \text{for } x_{ij} = y_{ij} \\ p_b & \text{for } x_{ij} = b \end{cases} \quad (1)$$

where a is the minimum intensity (dark dot); b is the

maximum intensity (light dot); p_a is the probability of intensity a generation; p_b is the probability of intensity b generation; p is the noise density, $p = p_a + p_b$; and y_{ij} is the intensity of the pixel at location (i, j) in the uncorrupted image.

If either p_a or p_b is zero the impulse noise is called unipolar noise. If neither probability is zero and especially if they are equal, impulse noise is called bipolar noise or salt-and-pepper noise.

The considered kind of noise is most commonly caused by malfunctioning CCD elements (i.e. hot and dead pixels) and flecks of dust inside the camera. It also creeps into the images because of bit errors in transmission, faulty memory locations and erroneous switching during quick transients.

3 Review of existing median-based filters

SMF is a well-established method for impulse noise removal [1, 5, 6]. Still because it is performed uniformly across the image it removes noise and desirable image details too.

As a remedy to disadvantages of SMF variety of median-based approaches have been proposed. In general, they can be divided into two main groups: (i) weighted median filters (WMF) and (ii) switching median filters.

WMF selectively give some weights to pixels in the filtering window usually with the central pixel contributing the most [9–11]. Higher weights assigned to the central pixel reduce smoothing effect and makes WMF better in preserving image sharpness [12–14]. However, similar to SMF, weighted median filtration is performed across all pixels in an image: corrupted and uncorrupted ones. This significantly affects quality of the output image. WMF will not be considered in this paper.

Switching (or decision based) median filters is a common name for a group of filters that reduce number of pixels subjected to median filtration to those that are believed to be noisy [15]. Pixels identified as uncorrupted are left unchanged. The main part of each switching filter is impulse noise detection method. Different approaches are incorporated in this stage.

Most commonly, for impulse detection local image statistics are used. They quantify how intensity of the certain pixel differs from its neighbours. Rank-ordered differences are often applied [16, 17]. Other sophisticated methods such as boundary discriminative noise detection (BDND) [18] or techniques based on the minimum absolute value of convolutions obtained using one-dimensional Laplacian operators presented in [19] have been proven to be successful in impulse noise detection.

Recently, fuzzy techniques and neural networks [20–23] have also become popular in determining which pixels should be subjected to median filtration.

Both types of indicated median filters can be noise adaptive that is adjust size of the filtering window to noise properties (most commonly to its density) [13, 14, 24–27].

From the point of view of the classification presented above, the proposed method is adaptive switching median filter. Its detailed description is given in the following section.

4 The proposed approach

The proposed approach to noise removal reduces number of pixels subjected to median filtration. The method contains switching mechanism which determines action that should be applied to consecutive pixels of the filtered image. Only

pixels identified as corrupted are subjected to median filtration. Uncorrupted pixels are left unchanged.

The general architecture of the proposed median filter is shown in Fig. 1.

4.1 Noise detection

In digital images impulse noise manifests itself as local intensity fluctuations. Corrupted pixels appear as single, isolated dots, significantly brighter or significantly darker than their neighbours. These pixels can be then considered as local extrema of intensity function. Pixels brighter than their neighbours are local intensity maxima and pixels darker than their neighbours are local intensity minima.

The proposed noise detection scheme is based on the idea presented above. It searches the image for local intensity extrema in order to decide whether the pixel is corrupted or uncorrupted. The search is performed in areas determined by square window which passes through the image pixel-by-pixel. In each window local intensity minima and local intensity maxima are determined. Location of the local intensity extrema is marked by increasing the corresponding values on maps of local extrema. This idea is presented in Fig. 2.

Complete maps of local extrema for example from Fig. 2 are presented in Fig. 3.

For the window of size $n \times n$ pixels, each pixel can be considered as a local intensity extremum n^2 times. It can be assumed that values on the maps of extrema determine 'the strength of the extremum'. The stronger the extremum, the more times pixel was identified as an extremum in the

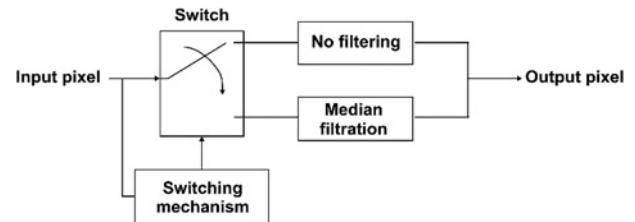


Fig. 1 General architecture of the proposed median filter

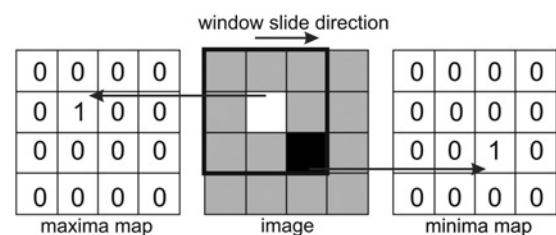


Fig. 2 Building maps of local intensity extrema using window of size 3×3 pixels

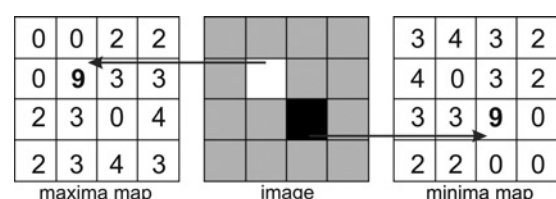


Fig. 3 Complete maps of local extrema for example from Fig. 2

0	0	0	0
0	1	0	0
0	0	1	0
0	0	0	0

Fig. 4 Binary decision map build for the example presented in Fig. 2

considered neighbourhoods. In presented implementation a pixel is considered noisy if it appears to be local extremum in n^2 number of windows. Especially, value of n^2 on minima map is supposed to indicate location of dark dots (pepper). Analogously, value of n^2 on maxima map is supposed to indicate location of light dot (salt).

In the proposed approach window of size 3×3 pixels is used. It was experimentally tested that bigger windows increase time of the algorithm performance without significant improvement in noise detection accuracy.

In the last step of the noise detection process binary decision map is build. 1's are set in all locations where values on minima map or maxima map equal to n^2 which is a squared window size. The remaining locations are filled with 0's. Pixels with 1's on binary decision map are considered corrupted and are subjected to median filtration. Pixels with 0's on binary decision map are considered uncorrupted and are left unchanged. The binary decision map for the example from Fig. 2 is shown in Fig. 4.

The proposed noise detection scheme can be summarised as follows:

1. Set zeros on map of local minima.
2. Set zeros on map of local maxima.
3. Impose 3×3 window centered on the current pixel.
4. In the window find local intensity minima and increase corresponding value on map of local minima.
5. In the window find local intensity maxima and increase corresponding value on map of local maxima.
6. Move window to the next pixel.
7. Repeat steps 3–6 until all pixels are checked.
8. For all locations where value on map of local minima or map of local maxima equals to squared window size (i.e. 9 in the considered implementation) set 1's on binary decision map, for remaining locations set 0's on binary decision map.

4.2 Filtering scheme

The filtering scheme was adapted from the filter with BDND method described in [18].

Filtering is performed based on binary decision map. Only pixels identified as corrupted (1's on binary decision map) are subjected to median filtration. Their new value is defined as a median value of uncorrupted pixels (0's on binary decision map) located in the window of size W_{D1} . Note that the current pixel is excluded from the median filtration as it is identified as corrupted. Window dimensions change in function of the noise density. The values of W_{D1} are given in Table 1. As stated in [18] they were empirically established based on multiple images.

Tests considering use of bigger windows for higher noise densities were also performed. Especially, window dimensions proposed in [24, 26] were considered. However, analysis of obtained results proved that dimensions given in Table 1 are sufficient. Increase in window size increases

Table 1 Suggested window size for estimated noise density level

Noise density	$W_{D1} \times W_{D1}$
$0\% < p \leq 20\%$	3×3
$20\% < p \leq 40\%$	5×5
$p > 40\%$	7×7

time of algorithm performance without significant improvement of image restoration efficiency.

The proposed method introduces slight changes into BDND filtering scheme. The source method starts with the smallest window (3×3) and iteratively extends it outward by one pixel in all four directions until (i) the number of uncorrupted pixels in the window area is less than a half of squared window size or (ii) maximum W_{D1} window size is reached.

The tests that we performed have proven that for highly corrupted images number of uncorrupted pixels in the window area hardly ever reaches a half of squared window size and in case of most pixels median filtration is performed using the maximum window size. Therefore the proposed approach resigns from iterative window resizing and uses constant window size depending on the noise density (in accordance with Table 1).

4.3 Noise density estimation

Many sophisticated methods for noise density estimation have been proposed for example quad-tree decomposition [24] peaks and valleys detection [28] or methods based on analysis of the first or the second derivation of the image [29].

In the proposed method noise density estimation was simplified. It is determined based on number of detected noisy pixels. 1's on binary decision map are counted and their number is divided by a total number of pixels in the considered image.

5 Image fidelity measures

The performance evaluation of noise removal using the proposed method was quantified by peak signal-to-noise ratio (PSNR) and structural SIMilarity (SSIM) index.

The PSNR was calculated using the standard formula given as follows

$$\text{PSNR} = 10 \log_{10} \left(\frac{L^2}{\text{MSE}} \right) \quad (2)$$

where L is the dynamic range of allowable intensities, MSE is the mean squared error, and

$$\text{MSE} = \frac{1}{MN} \sum_{i=1}^M \sum_{j=1}^N (y_{ij} - x_{ij})^2 \quad (3)$$

where M, N are the image dimensions (in pixels); y_{ij} is the intensity of pixel at location (i, j) in the original image; and x_{ij} is the intensity of pixel at location (i, j) in the filtered image.

Regardless their popularity, PSNR and MSE have been proven inadequate for perceptual evaluation of image degradations [30]. Therefore SSIM index [31] was applied as second image fidelity measure.



Fig. 5 Standard test images used for algorithm performance analysis

a Barbara
b Boat
c Goldhill

The SSIM index has been developed to improve on methods inconsistent with human eye perception. To explore structural information in an image it separates task of similarity measurement into three comparisons:

- luminance $l(x, y)$;
- contrast $c(x, y)$;
- structure $s(x, y)$;

in accordance with the following equation [31]

$$\text{SSIM}(x, y) = [l(x, y)]^\alpha [c(x, y)]^\beta [s(x, y)]^\gamma \quad (4)$$

where parameters $\alpha > 0$, $\beta > 0$, $\gamma > 0$ are used to adjust the importance of the components and $l(x, y)$, $c(x, y)$ and $s(x, y)$ are given by equations (5)–(7) respectively

$$l(x, y) = \frac{2\mu_x\mu_y + C_1}{\mu_x^2 + \mu_y^2 + C_1} \quad (5)$$

where μ_y , μ_x are the mean intensities of the original and restored image, respectively; and C_1 is the constant equal to $(K_1L)^2$, where $K_1 \ll 1$

$$c(x, y) = \frac{2\sigma_x\sigma_y + C_2}{\sigma_x^2 + \sigma_y^2 + C_2} \quad (6)$$

where σ_y , σ_x are the standard deviations of intensities in the original and restored image, respectively; and C_2 is constant equal to $(K_2L)^2$, where $K_2 \ll 1$

$$s(x, y) = \frac{\sigma_{xy} + C_3}{\sigma_x\sigma_y + C_3} \quad (7)$$

where σ_{xy} is the cross-correlation between the original and restored image and C_3 is the constant.

In accordance to suggestions given in [31] in this paper the following values of parameters were used: $\alpha = \beta = \gamma = 1$, $K_1 = 0.01$, $K_2 = 0.03$ and $C_3 = C_2/2$. Local SSIM indexes were computed using window size of 11×11 pixels passing throughout the image pixel-by-pixel. Local indexes were next averaged in order to compute global SSIM index. In case of ideal match of two images SSIM index equal to 1. Then, it decreases to 0 together with decreasing visual similarity between compared images.

6 Simulation results

The proposed filter was extensively tested on a different images corrupted by salt and pepper noise. Eight-bit monochromatic images under a wide range (from 5 to 98%) of noise corruption were considered. In this section, results obtained for standard test images [32, 33] are presented. Especially images of: Barbara, Boat and Goldhill are used. They are presented in Fig. 5. The size of each image was 512×512 pixels. Image quality is given by means of PSNR and SSIM index computed as described in the previous section. Marginal pixels on every side of the image were excluded from the image quality estimation.

6.1 The accuracy of noise detection

The crucial task while image denoising using the proposed algorithm is impulse noise detection and estimation of its density. Table 2 presents results of evaluation of noise detection accuracy for considered standard test images (i.e. Barbara, Boat and Goldhill) under a wide range of noise corruption. The evaluation is presented by means of:

- number of miss detections that is number of noisy pixels disregarded during noise detection [denoted as MD (pix)];
- percent of miss detections that is fraction of noisy pixels disregarded during noise detection in reference to real noise density p [denoted as MD (%)];
- number of over detections that is number of uncorrupted pixels identified as noisy during noise detection [denoted as OD (pix)]; and
- per cent of over detections that is fraction of uncorrupted pixels identified as noisy in reference to real noise density p [denoted as OD (%)].

The names of the images are indicated in column caption.

In Fig. 6 graphs illustrating accuracy of noise density estimation are presented. Again images of Goldhill, Barbara and Boat are considered. Fig. 6a shows the dependency between the real and the estimated noise density. In Fig. 6b the disparity between estimated and real noise densities in function of the real noise density is shown.

Results presented in Table 2 and Fig. 6 show clearly that the proposed method is very robust in impulse noise detection. The algorithm detects 100% of noisy pixels present in the corrupted image. For a wide range of noise corruption (5–98%), the number of misdetections equal to zero. The

Table 2 Evaluation of misdetections (MD) and overdetections (OD) resulted after applying the proposed noise detection scheme to exemplary noisy images corrupted under various noise densities

Noise, %	Noise, pix	Boat					Barbara				
		Detected noisy	MD, pix	MD, %	OD, pix	OD, %	Detected noisy	MD, pix	MD, %	OD, pix	OD, %
5	13 009	13 009	0	0.0	11 388	89.72	13 009	0	0.00	8621	67.92
10	26 014	26 014	0	0.0	6382	25.76	26 014	0	0.00	4842	19.56
20	52 028	52 028	0	0.0	1463	2.90	52 028	0	0.00	1122	2.22
30	78 019	78 019	0	0.0	390	0.51	78 019	0	0.00	307	0.40
40	104 066	104 066	0	0.0	72	0.07	104 066	0	0.00	67	0.07
50	130 057	130 057	0	0.0	6	0.00	130 057	0	0.00	9	0.01
60	156 070	156 070	0	0.0	5	0.00	156 070	0	0.00	1	0.00
70	182 088	182 088	0	0.0	2	0.00	182 088	0	0.00	0	0.00
80	208 057	208 057	0	0.0	0	0.00	208 057	0	0.00	0	0.00
90	234 090	234 090	0	0.0	0	0.00	234 090	0	0.00	0	0.00
98	254 900	254 900	0	0.0	0	0.00	254 900	0	0.00	0	0.00

Noise, %	Noise, pix	Goldhill				
		Detected noisy	MD, pix	MD, %	OD, pix	OD, %
5	13 009	13 009	0	0.00	37 158	285.68
10	26 014	26 014	0	0.00	17 158	69.03
20	52 028	52 028	0	0.00	6453	13.67
30	78 019	78 019	0	0.00	1177	1.53
40	104 066	104 066	0	0.00	259	0.24
50	130 057	130 057	0	0.00	33	0.02
60	156 070	156 070	0	0.00	4	0.00
70	182 088	182 088	0	0.00	1	0.00
80	208 057	208 057	0	0.00	0	0.00
90	234 090	234 090	0	0.00	0	0.00
98	254 900	254 900	0	0.00	0	0.00

significant number of overdetections (pixels erroneously identified as noisy) appear only in case of images with slight level of noise corruption ($p < 10\%$). For highly corrupted images, the number of overdetections rapidly decrease and can be neglected for noise densities higher than 30%.

The significant number of overdetections for low noise densities is caused by the fact that in case of noise-free neighbourhood even one level of difference in image intensity is considered by the proposed noise detection scheme as a local intensity extremum. If the aim of the algorithm is to remove only impulse noise this effect should

be considered as a disadvantage. On the other hand, it makes the method sufficient for removal of random-valued impulse-like noise.

The efficiency of noise detection makes simplified noise density estimation very accurate. The dependency between real and estimated densities is almost linear especially for noise densities higher than 20% (see Fig. 6a). For noise densities lower than 20%, the disparity between real and estimated noise density is less than 5%. This difference does not influence the window size selection during the filtration process.

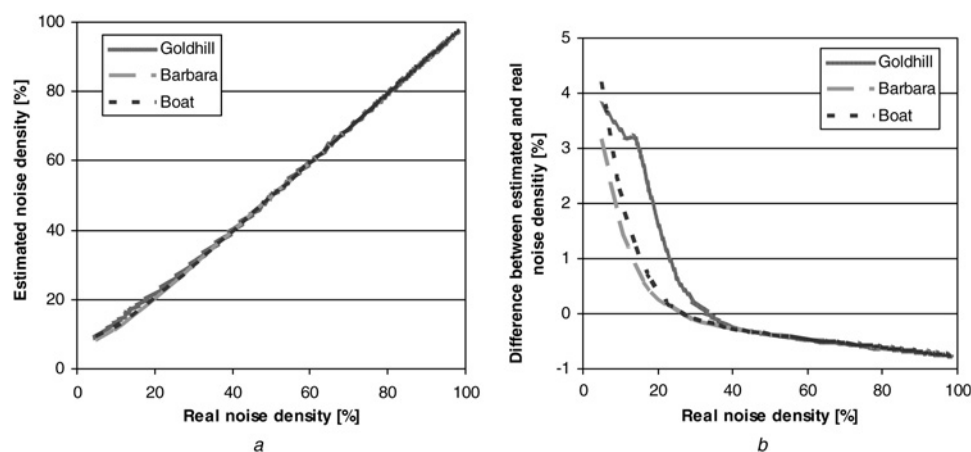


Fig. 6 Accuracy of noise density estimation for test images under a wide range of noise corruption

a Estimated noise density in function of real noise density

b The disparity between estimated and real noise densities in function of the real noise density







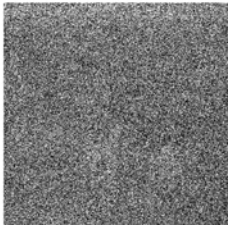

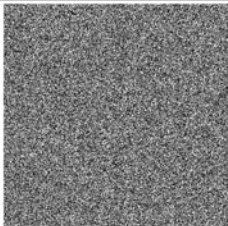

NOISY IMAGE		DENOISED IMAGE	
$p=20\%$ PSNR= 12.80 dB SSIM = 0.14			PSNR = 31.50 dB SSIM = 0.96
$p=40\%$ PSNR = 9.39 dB SSIM = 0.05			PSNR = 27.66 dB SSIM = 0.90
$p=60\%$ PSNR= 7.64 dB SSIM = 0.03			PSNR = 25.26 dB SSIM = 0.81
$p=80\%$ PSNR = 6.33 dB SSIM= 0.01			PSNR = 23.50 dB SSIM = 0.70
$p=98\%$ PSNR = 5.44 dB SSIM = 0.00			PSNR = 17.28 dB SSIM = 0.38

Fig. 7 Results of noise removal from Goldhill image using the proposed method

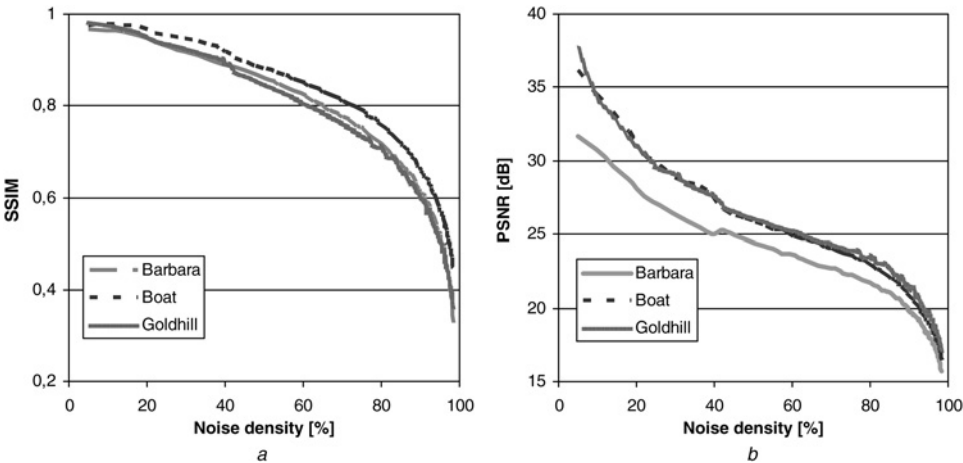


Fig. 8 Changes of the denoised image in function of noise density in the corrupted image

a PSNR
b SSIM index

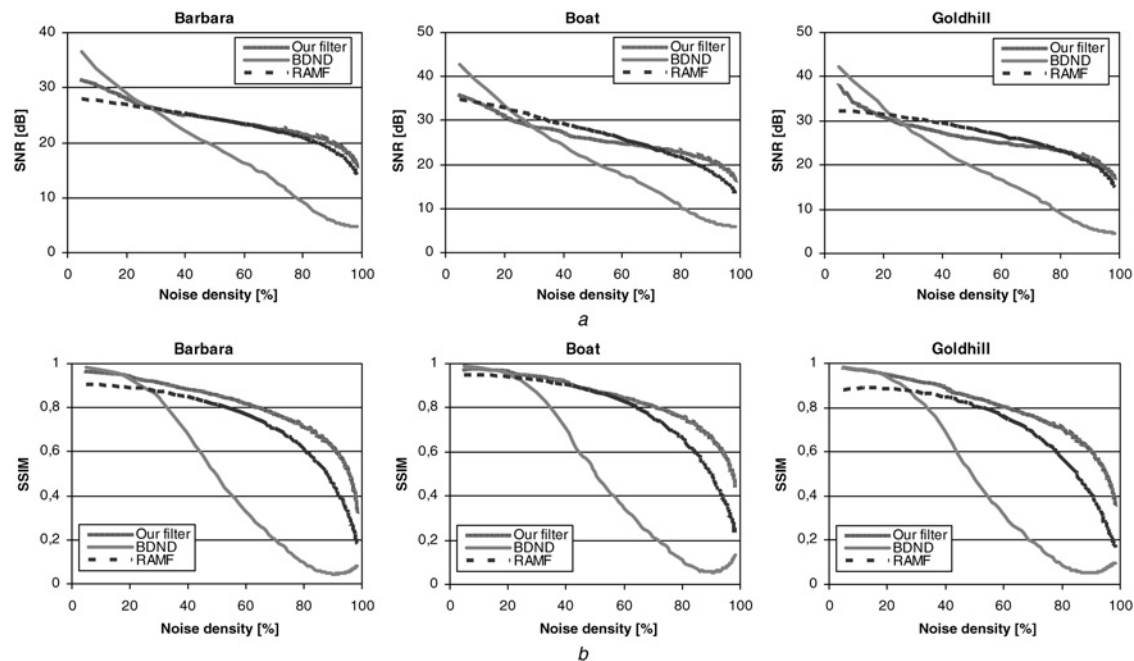


Fig. 9 Performance comparison of the proposed method, switching median filter with BDND incorporated and ranked-order median filter (RAMF)

a Comparison by means of PSNR
b Comparison by means of SSIM index The name of the image is indicated on each graph

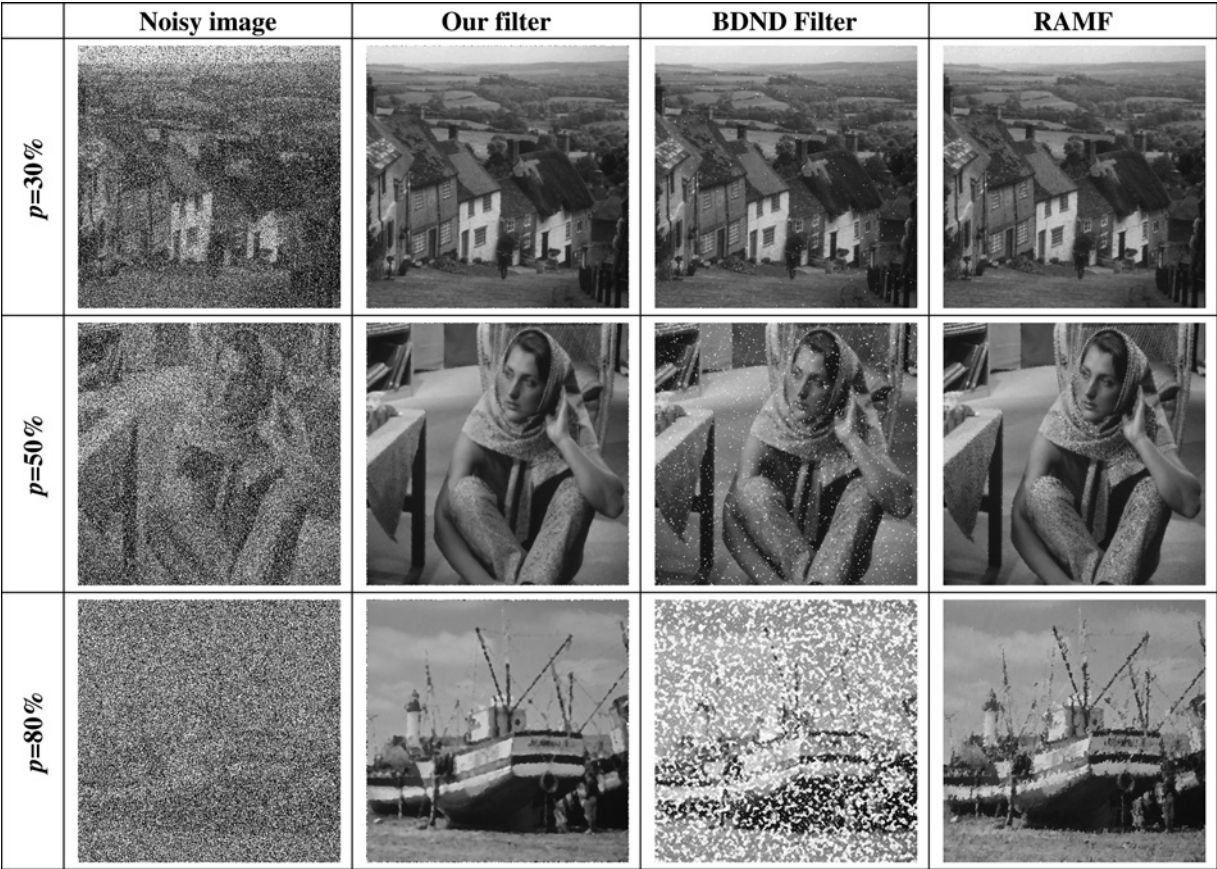


Fig. 10 Results of denoising corrupted images of Goldhill, Barbara and Boat using the proposed method (second column), switching median filter with BDND incorporated (third column) and RAMF (fourth column)

Impulse noise density is indicated at the beginning of the each row

6.2 Noise removal efficiency

In Fig. 7 results of noise removal from noise-corrupted Goldhill image is shown. Noisy images are presented on the left. Images after restoration using the proposed method are shown on the right side. Noise density p and values of PSNR and SSIM index are indicated next to each image.

Fig. 8 shows graphs presenting changes of PSNR (Fig. 8a) and SSIM index (Fig. 8b) in the denoised image in function of noise density in the corrupted image. Images of Goldhill, Boat and Barbara are considered.

Results presented in Fig. 9 show that the proposed filter can successfully restore images under a wide range of noise corruption. Together with increasing noise density some fine details are lost in the restoration process (values of PSNR and SSIM decrease). However, even in case of noise densities close to 90% the method provides visually pleasing output. This is proved by high values of SSIM index (see Fig. 8a). Even if 98% of an image is corrupted by noise, the original objects can be distinguished in the restored image.

7 Comparison with existing approaches

In this section results obtained by the proposed filter are compared with results provided by well-established methods for impulse noise removal. Especially, the switching median filter with BDND [18] and the ranked-order-based adaptive median filter (RAMF) [15] are considered. The comparison is made by means of PSNR (Fig. 9a) and SSIM index (Fig. 9b). Images of Goldhill, Boat and Barbara are considered. The name of the image is indicated on each graph.

Visualisation of results obtained by the considered methods for different impulse noise densities is given in Fig. 10. First column presents noise-corrupted image. The noise density p is indicated on the left side. Second column presents results of image denoising using the proposed filter. The third column shows images restored using switching median filter with BDND incorporated. Finally in the last column results of noise removal using the RAMF are presented.

Results presented in Figs. 9 and 10 show that the proposed method outperforms well-established methods for impulse noise removal. Especially in case of highly corrupted images superiority of the new filter can be seen.

Although PSNR obtained for noise corruption level lower than 20% is slightly better for images denoised using BDND filter there are significant noise blotches in the restored images. The blotches deteriorate visual quality of the image what is proven by lower values of SSIM index. For high noise densities ($p > 80\%$) results obtained using the proposed filter are far superior to results obtained using BDND. The superiority of the proposed filter is confirmed by PSNR and SSIM index.

For a wide range of noise corruption values of PSNR obtained by the new method are very similar to those provided by RAMF. However, SSIM indexes of images recovered by the new method are always higher than those of ranked-order median filter. This means that the proposed approach is more robust in preserving details and ensures more visually pleasing output.

8 Conclusions

In this paper problem of image denoising was considered. Particular attention was paid to impulse noise removal. A median-based switching filter was proposed. The filter utilises very robust and accurate noise detection scheme. Its

main idea is to locate local minimum and maximum in each window. Then a pixel is considered noisy if it appears to be local extremum in more than a fixed number of windows. In consequence, noise corrupted pixels can be effectively removed while preserving the detailed image information at the same time.

Results of extensive simulations were presented. Results of the new method were compared with those obtained by well-established methods for impulse noise removal. Analysis of the results reveals that the proposed algorithm consistently outperforms well-established methods. For a wide range of noise corruption (5–98%) it provides high-quality results comprehensible in overall image contents. The introduced method is especially robust in restoration of images under a high noise density. Therefore the algorithm can be successfully applied for restoration of extremely corrupted images.

In the case of low and medium noise densities the proposed method of noise removal is faster than the SMF because only those pixels classified as noise corrupted are processed. However the quality may be somewhat lower because the classification of pixels is not perfect. The number of correctly classified noisy pixels subjected to median filtration increases with noise density. The cost of the proposed method therefore increases with noise density but there is a significant performance advantage in terms of both cost and PSNR over existing techniques.

9 Acknowledgment

Anna Fabijańska is a scholarship holder of project entitled 'Innovative education ...' supported by European Social Fund.

10 References

- Gonzalez, R.C., Woods, R.E.: 'Digital image processing' (Prentice Hall, 2007, 3rd edn.)
- Arce, G.R., Gallagher, N.C., Nodes, T.: 'Median filters: theory and applications', in HUANG, T. (Ed.): 'Advances in computer vision and image processing' (JAI, Connecticut 1986)
- Pitas, I., Venetsanopoulos, A.N.: 'Nonlinear digital filters principles and applications' (Kluwer, 1990)
- Astola, J., Kuosmanen, P.: 'Fundamentals of nonlinear digital filtering' (CRC Press, 1997)
- Pitas, I., Venetsanopoulos, A.N.: 'Order statistics in digital image processing', *Proc. IEEE*, 1992, **80**, (12), pp. 1893–1921
- Gil, J., Werman, M.: 'Computing 2-D min, median, and max filters', *IEEE Trans. Pattern Anal. Mach. Intell.*, 1993, **15**, (5), pp. 504–507
- Guangjin, Z., Jiegu, L.: 'Some problems of 2D morphological and median filters', *J. Shanghai Univ. (English Edition)*, 1997, **1**, (3), pp. 245–248
- Nodes, T.A., Gallagher, Jr. N.C.: 'The output distribution of median type filters', *IEEE Trans. Commun.*, 1984, **COM-32**, pp. 532–541
- Brownrigg, D.: 'The weighted median filter', *Comm. Assoc. Comput.*, 1984, **27**, (8), pp. 807–818
- Yin, L., Yang, R., Gabbouj, M., Neuvo, Y.: 'Weighted median filters: a tutorial', *IEEE Trans. Circuits Syst.*, 1996, **43**, (3), pp. 157–192
- Zhou, H., Zeng, B., Neuvo, Y.: 'Weighted FIR median hybrid filters for image processing'. Proc. Int. Conf. on Circuits and Systems, Shenzhen, China, 1991, pp. 793–796
- Ko, J., Lee, J.-H.: 'Center weighted median filters and their application to image enhancement', *IEEE Trans. Circuits Syst.*, 1991, **38**, (9), pp. 984–993
- Chen, T., Wu, H.R.: 'Adaptive impulse detection using center-weighted median filters', *IEEE Signal Process. Lett.*, 2001, **8**, (1), pp. 1–3
- Chan, R.H., Chen Hu Nikolova, M.: 'An iterative procedure for removing random-valued impulse noise', *IEEE Signal Process. Lett.*, 2004, **11**, (12), pp. 921–924

- 15 Hwang, H., Haddad, R.A.: 'Adaptive median filters: new algorithms and results', *IEEE Trans. Image Process.*, 1995, **4**, (4), pp. 499–502
- 16 Garnett, R., Huegerich, T., Chui, C., He, W.: 'Universal noise removal algorithm with an impulse detector', *IEEE Trans. Image Process.*, 2005, **14**, (11), pp. 1747–1754
- 17 Abreu, E., Lightstone, M., Mitra, S.K., Arakawa, K.: 'A new efficient approach for the removal of impulse noise from highly corrupted images', *IEEE Trans. Image Process.*, 1996, **5**, (6), pp. 1012–1025
- 18 Ng, P.-E., Ma, K.-K.: 'A switching median filter with boundary discriminative noise detection for extremely corrupted images', *IEEE Trans. Image Process.*, 2006, **15**, (6), pp. 1506–1516
- 19 Zhang, S., Karim, M.A.: 'A new impulse detector for switching median filters', *IEEE Signal Process. Lett.*, 2002, **9**, (11), pp. 360–363
- 20 Zvonarev, P.S., Apalkov, I.V., Khryashchev, V.V., Reznikova, I.V.: 'Neural network adaptive switching median filter for the restoration of impulse noise corrupted images', *Lect. Notes. Comput. Sci.*, 2005, **3656/2005**, pp. 223–230
- 21 Toprak, A., Güler, İ.: 'Suppression of impulse noise in medical images with the use of fuzzy adaptive median filter', *J. Med. Syst.*, 2006, **30**, (6), pp. 465–471
- 22 Lee, C., Guo, S., Hsu, C.: 'A novel fuzzy filter for impulse noise removal', *Lect. Notes. Comput. Sci.*, 2004, **3174/2004**, pp. 375–380
- 23 Patino-Escarcina, R.E., Costa, J.A.F.: 'An evaluation of MLP neural network efficiency for image filtering'. Proc. Seventh Conf. on Intelligent Systems Design and Applications, Rio de Janeiro, Brazil, 2007, pp. 335–340
- 24 Eng, H.-L., Ma, K.-K.: 'Noise adaptive soft-switching median filter', *IEEE Trans. Image Process.*, 2001, **10**, (2), pp. 242–251
- 25 Lin, H.M., Wilson, Jr. A.N.: 'Median filters with adaptive length', *IEEE Trans. Circuits Syst.*, 1988, **35**, (6), pp. 675–690
- 26 Vijaykumar, V.R., Vanathi, P.T., Kanagasabapathy, P., Ebenezer, D.: 'High density impulse noise removal using robust estimation based filter', *IAENG Int. J. Comput. Sci.*, 2008, **35**, (3), pp. 259–266 available on-line at: http://www.iaeng.org/IJCS/issues_v35/issue_3/index.html, accessed July 2009
- 27 Lee, Y., Takahashi, N., Tsai, D., Ishii, K.: 'Adaptive partial median filter for early CT signs of acute cerebral infarction', *Int. J. Comput. Assist. Radiol. Surg.*, 2007, **2**, (2), pp. 105–115
- 28 Windyga, P.S.: 'Fast impulsive noise removal', *IEEE Trans. Image Process.*, 2001, **10**, (1), pp. 173–179
- 29 Immerkaer, J.: 'Fast noise variance estimation', *Comput. Vis. Image Understand.*, 1996, **64**, (2), pp. 300–302
- 30 Wang, Z., Bovik, A.C.: 'Mean squared error: love it or leave it', *IEEE Signal Proc. Mag.*, 2009, **26**, (1), pp. 98–117
- 31 Wang, Z., Bovik, A.C., Sheikh, H.R., Simoncelli, E.P.: 'Image quality assessment: from error visibility to structural similarity', *IEEE Trans. Image Process.*, 2004, **13**, (4), pp. 600–612
- 32 <http://decsai.ugr.es/cvg/CG/base.htm>, accessed July 2009
- 33 <http://sipi.usc.edu/database/>, accessed July 2009